Hydrodynamic study of phase-shift tidal power system with Y-shaped dams

Article *in* Journal of Hydraulic Research · June 2014

DOI: 10.1080/00221686.2013.875071

CITATIONS
2

READS
93

2 authors, including:

Qiulin Liu
National Marine Data and Information Service, State Oceanic Administration, China
11 PUBLICATIONS **28** CITATIONS

SEE PROFILE

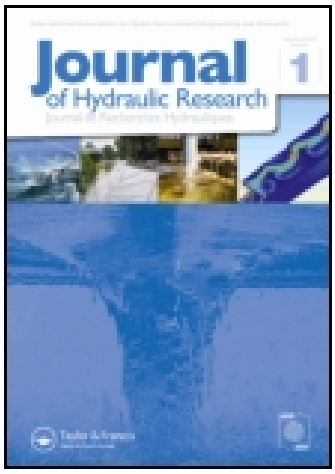

Journal of Hydraulic Research
Publication details, including instructions for authors and subscription information:
http://www.tandfonline.com/loi/tjhr20

Hydrodynamic study of phase-shift tidal power system with Y-shaped dams

Qiulin Liu[a] & Yongliang Zhang[b]

[a] PhD Student, State Key Laboratory of Hydroscience and Engineering, Tsinghua University, Beijing 100084, People's Republic of China

[b] Professor, State Key Laboratory of Hydroscience and Engineering, Tsinghua University, Beijing 100084, People's Republic of China

Published online: 30 Apr 2014.

IAHR AIRH
Taylor & Francis
Taylor & Francis Group

Journal of Hydraulic Research Vol. 52, No. 3 (2014), pp. 356–365
http://dx.doi.org/10.1080/00221686.2013.875071

Research paper

Hydrodynamic study of phase-shift tidal power system with Y-shaped dams

QIULIN LIU, PhD Student, *State Key Laboratory of Hydroscience and Engineering, Tsinghua University, Beijing 100084, People's Republic of China*
Email: liuql11@mails.tsinghua.edu.cn

YONGLIANG ZHANG, Professor, *State Key Laboratory of Hydroscience and Engineering, Tsinghua University, Beijing 100084, People's Republic of China*
Email: yongliangzhang@mail.tsinghua.edu.cn (author for correspondence)

ABSTRACT
Phase-shift tidal power system with a dam deployed perpendicularly to a coastline in the sea is considered. The tidal power is extracted from water level difference on both sides of the dam, which originates from different propagation path of the tidal wave and the phase shift in water levels. This study focuses on hydrodynamic characteristics of a Y-shaped dam under the action of the tidal waves and explores the effects of the dam parameters on the phase shift of the tidal waves on both sides of a main dam and water head. A two-dimensional model is used to simulate tidal flows in the Taiwan Strait and Qiongzhou Strait. The model is validated by comparing the numerical results with previous studies and available measurements. The influence of the angle between the main dam and the branch dam, branch dam length, and dam types on phase difference in water levels and water head over the main dam is discussed.

Keywords: Hydrodynamic characteristics; phase-shift tidal power; two-dimensional model; water head; Y-shaped dam

1 Introduction

Traditional tidal power originates from the potential energy of water level difference caused by ebb and flood tides and is extracted by constructing a barrage across an estuary or the mouth of a bay in coastal waters to form a basin. Although electricity generation of such a tidal power has been put into service widely for decades all over the world, it still faces big challenges in the following aspects: very high construction costs, negative ecological and environmental impacts (such as sediment deposition, damage to estuarine ecosystems, threat to feeding and breeding areas for wildlife, reduction in the self-purification capacity of water body), obstruction of water transportation, while relatively limited dam sites would be expected to produce considerable amounts of electricity with a competitive price. Therefore, for the pursuit of lower negative eco-environmental impact and more cost effectiveness, construction of a tidal power station needs to consider the above-mentioned factors. Such a tidal power development technology by utilizing tidal barrages across an estuary or the mouth of a bay area seems to become outdated and may be superseded by a more advanced technology of tidal power development, such as one by constructing a tidal dam perpendicular to the coastline to make use of dynamic tidal power (hereinafter called DTP) thereby avoiding a basin.

The concept of the DTP was presented by Hulsbergen *et al.* (2005, 2008), which involves creating a long dam-like structure perpendicular to the coastline, with an option for a coast-parallel branch barrier at the far end forming a large "T" shape. The dam would interfere with local tidal dynamics, creating water level differences on both sides of the dam and providing considerable water head over the dam. The numerical simulations on I- and T-shaped dams, with some openings along the dam to insert turbines, were conducted. The peak powers generated for a certain dam were calculated and showed in Table 1 (Hulsbergen *et al.* 2008). The results showed that the costing might be as low as 0.015€ per kilowatt-hour, close to the costing of ordinary hydraulic generation, showing a great potential to be harnessed.

Recently, a numerical simulation of tidal flow was also conducted in 22 sites viable for the construction of DTP dams along the Chinese coastline (Adema and Hartsuiker 2010). The maximum water head could be 3 m in certain sites, and if turbines are inserted, a 20 GW peak power would be gained. Results revealed

Received 31 January 2013; accepted 10 December 2013/Open for discussion until 31 December 2014.

ISSN 0022-1686 print/ISSN 1814-2079 online
http://www.tandfonline.com

Table 1 Peak power (MW) for square* T-dams with different dam length

	Maximum velocity (ms^{-1})				
Dam length (km)	0.60	0.80	1.00	1.20	1.40
10	235	362	505	664	837
15	647	997	1393	1831	2307
25	2321	3574	4995	6566	8274
35	5384	8289	11,584	15,227	19,188
45	10,091	15,536	21,712	28,541	35,966

Note: Square* means that the length of coast-perpendicular stem of the T-shaped dam is identical to the length of coast-parallel branch barrier of the dam.

that ideal sites with highest water heads include the Taiwan Strait, Yellow Sea, and the Qiongzhou Strait. A previous numerical study of T-shaped dams located in a specific location (namely Dalian, Liaotung Peninsula in the Bohai Sea) showed that the longer the coast-perpendicular dam or coast-parallel barrier was, the higher the water head was (Zheng *et al*. 2012).

All these efforts were confined to studying hydrodynamic characteristics for I- and T-shaped dams mainly in terms of water head. Based on the previous study (Zheng *et al*. 2012), phase-shift tidal power (PSTP) is presented, in which water head originates from phase shift of the tidal waves on both sides of the dam. The shift is caused by the different path of the tidal wave propagation. That is to say that if tide on one side of a dam rises to the highest level and the other side down to the lowest one, there should be the maximum tidal range, i.e. the largest water head. Although hydrodynamic characteristics for the I- and T-shaped dams were well investigated, all these studies have been conducted without consideration of the tidal wave gathering effects, usually related to the gradually narrowing geometry of a particular structure or topography. Therefore, it is necessary to consider a Y-shaped dam which has tidal wave gathering effects.

This paper extends the previously mentioned hydrodynamic characteristics study on PSTP for T-shaped dams, discussed by Zheng *et al*. (2012), by considering the effect of angle between a main dam and a branch dam, branch dam length and dam type on phase shift of the tidal waves and water head over the main dam. The objective is generally to understand the basic relations between the phase shift of the tidal waves and the water head, to investigate the effect of different geometrical parameters of the Y-shaped dam, and to optimize Y-shaped dams so as to obtain the maximum water head converted into power. In this work, we limit our attention to the effect of geometric parameters on water head and phase shift of the tidal waves on the both sides of the dam, and use a two-dimensional tidal wave model to simulate tidal flow in the Taiwan Strait and Qiongzhou Strait. The model is validated by comparing the numerical results with previous ones and measured ones. The influence of geometrical parameters of a Y-shaped dam and dam types on hydrodynamic characteristics is discussed.

2 Formulation of the problem

As described in the previous section, the Taiwan Strait site and the Qiongzhou Strait site along the Chinese coastline are ideal ones for constructing T-shaped PSTP dams. To maximize the tidal power generation, such two sites (hereinafter called Locations 1 and 2, respectively) are chosen as shown in Fig. 1. Hydrodynamic behaviours for PSTP of Y-shaped dams located in these two locations are explored.

For this purpose, we consider a symmetrical Y-shaped dam consisting of a main dam of length l and a branch dam of length L, deployed in the sea, where tidal currents run more or less

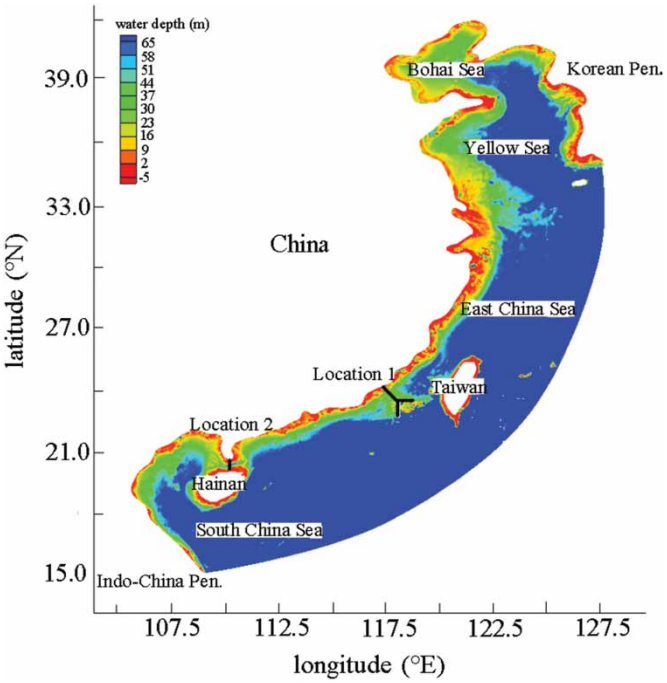

Figure 1 Investigation area with dams located in locations 1 and 2

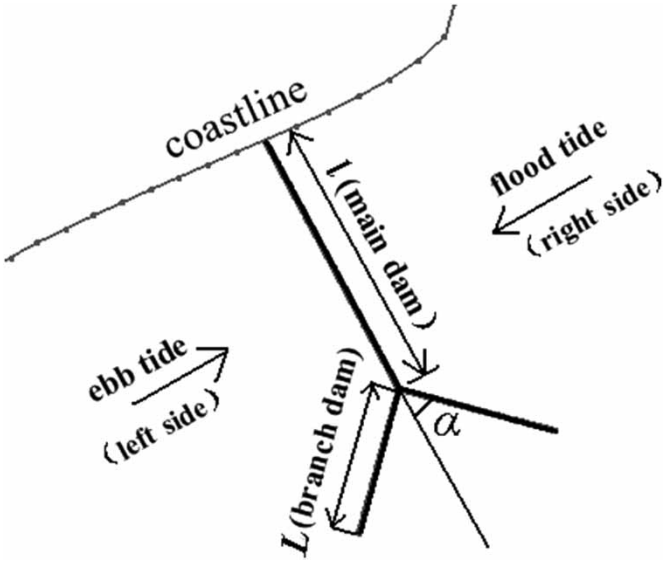

Figure 2 Y-shaped dam configuration

parallel to the coastline, as shown in Fig. 2. The main dam is perpendicular to the coastline. The angle between the main dam axis extension line and branch dam axis is α.

Since water depth in the area of investigation is small compared with horizontal scale in this study, a two-dimensional tidal flow model is applied. The hydrodynamic problem of tidal flow around the Y-shaped dam is formulated in a Cartesian coordinate system (x, y), and the fluid is described by the depth-average horizontal velocity filed (U, V).

The governing equations consist of the primitive continuity equation

$$\frac{\partial \zeta}{\partial t} + \frac{\partial Q_x}{\partial x} + \frac{\partial Q_y}{\partial y} = 0 \tag{1}$$

and the primitive momentum equations (in neoconservative form)

$$\frac{\partial U}{\partial t} + U\frac{\partial U}{\partial x} + V\frac{\partial V}{\partial y} - fV = -\frac{\partial}{\partial x}\left[\frac{P_S}{\rho_0} + g\zeta - g(\eta+\gamma)\right] + \frac{\tau_{sx}}{\rho_0 H} - \frac{\tau_{bx}}{\rho_0 H} + D_x - B_x \tag{2}$$

$$\frac{\partial V}{\partial t} + U\frac{\partial V}{\partial x} + V\frac{\partial V}{\partial y} + fU = -\frac{\partial}{\partial y}\left[\frac{P_S}{\rho_0} + g\zeta - g(\eta+\gamma)\right] + \frac{\tau_{sy}}{\rho_0 H} - \frac{\tau_{by}}{\rho_0 H} + D_y - B_y \tag{3}$$

where ζ is the free surface departure from the geoid, t is the time, H is the total water column thickness, Q_x and Q_y are the x- and y-directed fluxes per unit width, respectively, f is the Coriolis parameter, P_S is the atmospheric pressure at the sea surface, ρ is the time and spatially varying density of water due to salinity and temperature variations and ρ_0 is the reference density of water, g is the gravitational acceleration, η is the Newtonian equilibrium tide potential, γ is the earth tide, self-attraction and load tide, τ_{sx} and τ_{sy} are the imposed surface stress components, τ_{bx} and τ_{by} are the bottom stress components, D_x and D_y are the lateral stress gradients in the x- and y-direction, respectively, B_x and B_y are the baroclinic pressure gradients in the x- and y-direction, respectively.

The investigation area encompasses the entire Chinese coastline north to North Korea and south to Vietnam and the islands including Taiwan Island, Hainan Island and Jeju Island, as shown in Fig. 1. The GEBCO_08 database on land topography and ocean bathymetry data is used, which came from the report *Potential location for dynamic tidal power in China* (Adema and Hartsuiker 2010).

The land boundary is controlled by the wetting and drying parameters, mainly the water depth and velocity, while the ocean boundary is defined by the tidal components. Thirteen short-period constituents are applied to define the open ocean boundary including the principal lunar, principal solar, lunar-solar, elliptical solar, elliptical lunar constituents and they are derived from the TOPEX/POSEIDON satellite altimeter data (Matsumoto *et al*. 2000). Due to the arch open boundaries of the ocean, the known astronomic tidal components along the certain curve are then linear interpolated to suit the boundaries. By literature demonstration, the application of the components to the numerical simulation is feasible.

3 Results and discussion

Equations 1–3 together with their boundary conditions are solved using the Galerkin finite elements for spatial discretization and three level finite differences for time discretization, described in detail by Westerink *et al*. (1994) and Luettich and Westerink (2004). Calculations are carried out to test the model on I- and T-shaped dams, aiming to validate the model by comparing with the previous results and measured ones and then apply it to situations which have not been previously investigated. The influence of branch dam length L and angle α is analysed, and the effect of dam type is also examined. Numerical simulation of the tidal waves from 28 January to 5 February 2010 is carried out.

3.1 *Convergence analysis*

Prior to validating the model, a convergence analysis is conducted in order to determine element number and time step required. To this end, several typical points are chosen to examine the variation of water level and flow velocity in these points with time step and element number. Since results at all these typical points are similar, just the results at one point are given and shown in Figs. 3 and 4 for conciseness. It can be seen from Figs. 3 and 4 that stability is achieved when 50,000 or more finite elements and 10 s or longer time steps are used for the fluid domain. In this study, convergence was assumed when the relative error is less than 0.2%. All subsequent calculations were therefore carried out using 50,000 finite elements and 10 s time step for the fluid domain.

3.2 *Model validation*

To illustrate the validation of the present model, two examples are given of calculations of water heads acted over a I-shaped dam with dam length of 50 km at Locations 1 (Dongshan Island near Xiamen) and 2 (Qiongzhou Strait near Haikou) and a T-shaped dam at Location 1 with dam lengths of 50 and 100 km, together with another example of calculation of water levels in

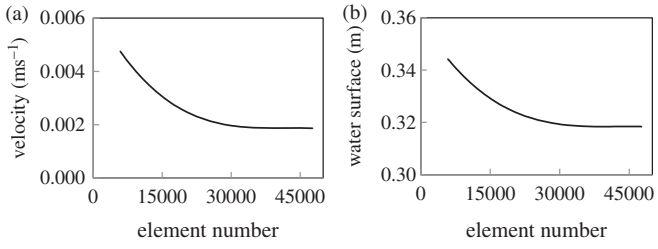

Figure 3 Variation of fluid parameters with element number: (a) flow velocity and (b) water surface level

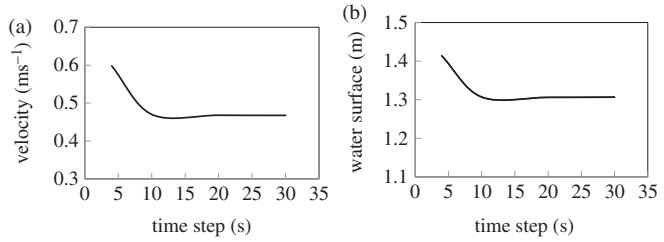

Figure 4 Variation of values with time step: (a) flow velocity and (b) water surface level

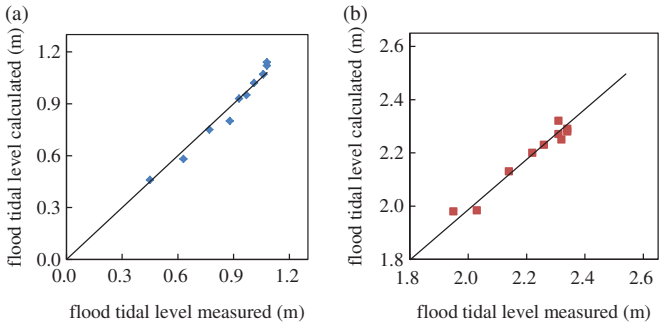

Figure 5 Comparisons of flood tidal level: (a) Dalian Station and (b) Xiamen Station

the absence of any dam. The tidal waves from 28 January to 5 February 2010 are considered. The optional branches of the T-shaped dams have a length of 50 km.

As this study focuses on water head and phase shift of the tidal waves on both sides of the dam, numerical results of water surface levels at the both sides of the dam becomes critical ones which are compared with the existing ones. As measured results of water levels in the presence of I-and T-shaped dam are not available, we start with the calculation of tidal levels in the absence of dam and then compared these numerical results with existing measured ones, which are from the National Bureau of Oceanography. The flood tidal levels for Dalian and Xiamen stations through 1–5 March 2011 are compared in Fig. 5. It can be seen from Fig. 5 that there is a good agreement between the numerical and measured ones.

In the following calculations in the presence of dam, for convenience of comparison a definition is introduced (see Fig. 2) as follows: the side facing flood tide is called as the right side and the side facing the ebb tide is called as the left side.

In the second example water levels at the both sides of the I-shaped dam ($l = 50$ km) at two different locations and water heads are compared with the existing results (Adema and Hartsuiker 2010). Figures 6 and 7 show the variations of water levels and water level differences with time for 50 km I-shaped dams. The water head is defined as the absolute difference between water levels on the both sides of the dam. Through the comparison shown in these two figures, it can be seen that the present results of water level, tidal wave phase, and period are in agreement with the previous ones (Adema and Hartsuiker 2010).

Table 2 shows the comparison of the present maximum water heads with the previous ones (Adema and Hartsuiker 2010). It

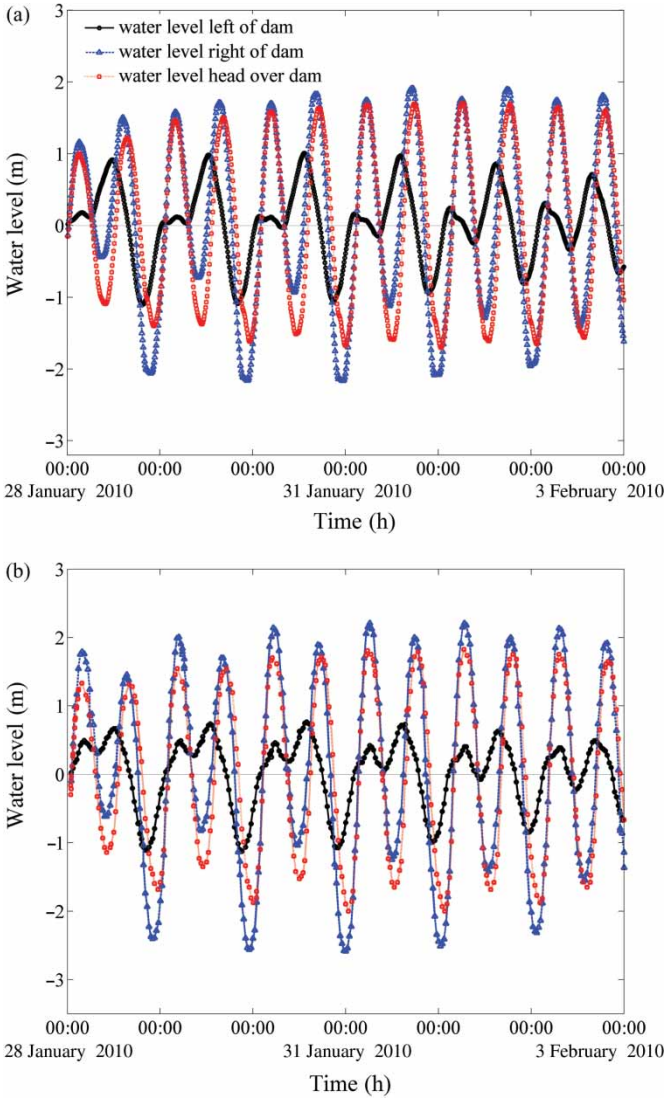

Figure 6 Variation of water level with time for 50 km I-shaped dam at Location 1: (a) present results and (b) previous results (Adema and Hartsuiker 2010)

can be seen that for I-shaped dam at Location 1 or Location 2, the present maximum water heads are slightly less than the previous ones. The relative differences of the maximum water heads are $E = 7.1\%$ and 13.9% during flood tide, for Locations 1 and 2, respectively, whereas the relative differences of the maximum water heads are $E = 14.6\%$ and 3.5% during ebb tide, E being defined as

$$E = \frac{|H_{m,2} - H_{m,1}|}{H_{m,1}} \tag{4}$$

where $H_{m,1}$ and $H_{m,2}$ are the maximum water heads in the previous and present study, respectively. Such big differences are probably due to the use of different scale nautical charts.

The third example examines the effect of dam length on water heads acted over T-shaped dam at Location 1. Figures 8 and 9 show the temporal variation of water level for T-shaped dams with two different dam lengths at Location 1. Similarly, through the comparison, it can also be seen that the present results of

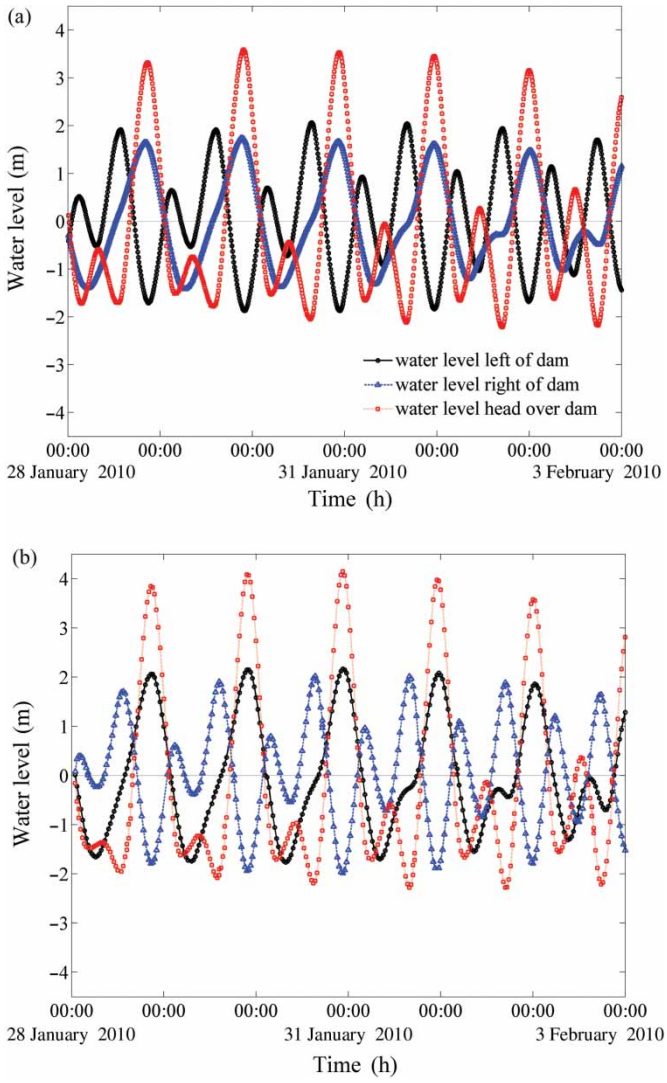

Figure 7 Variation of water level with time for 50 km I-shaped dam at Location 2: (a) present results and (b) previous results (Adema and Hartsuiker 2010)

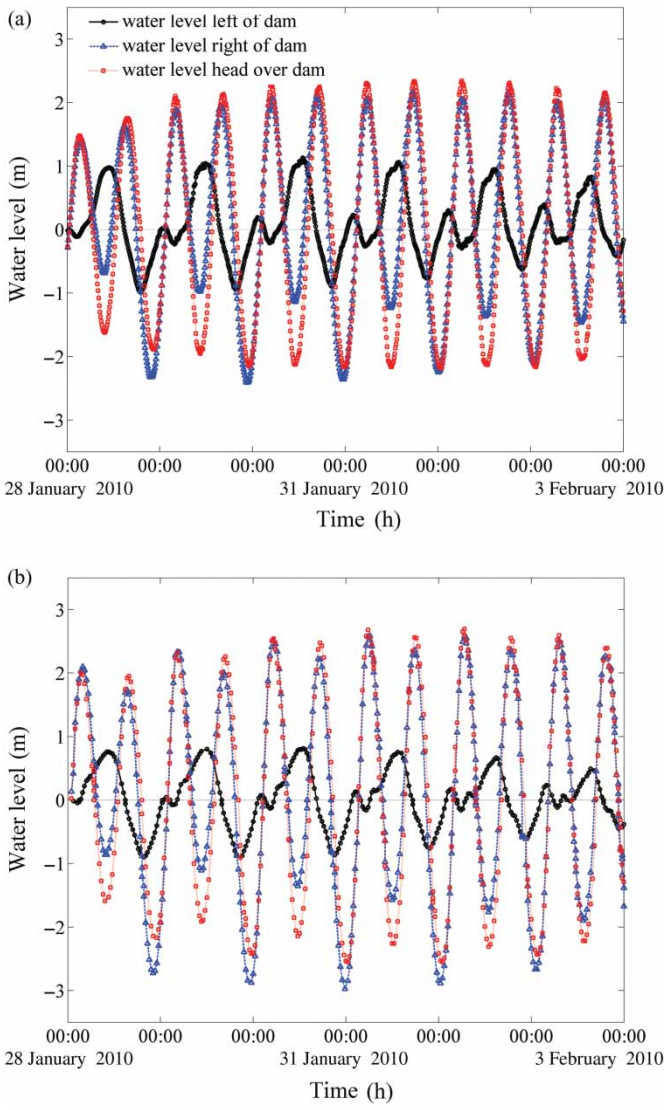

Figure 8 Variation of water level with time for 50 km T-shaped dam at Location 1: (a) present results and (b) previous results (Adema and Hartsuiker 2010)

water level, tidal wave phase, and period are in agreement with the previous ones. Results from Figs. 8 and 9 reveal that, the larger the main dam length is, the larger the water head is, as expected. The relative differences of the maximum water heads are 13.6% and 8.3% during flood tide for the 50 and 100 km long T-shaped dams, respectively, whereas the relative differences of the maximum water heads are 14.8% and 15.8% during ebb tide for Locations 1 and 2, respectively, as shown in Table 2.

3.3 *Frequency-domain analysis*

Given the good agreement between the existing results and present ones obtained using the model given in Section 2, a further analysis is necessary prior to presenting the results of our parametric study, in order to understand the difference in the behaviour of tidal waves between in the presence and absence of a dam.

Table 2 Comparison of the present maximum water heads with the previous ones (Adema and Hartsuiker 2010)

			Flood tide			Ebb tide		
Dam type	Site	Length	$H_{m,1}$ (m)	$H_{m,2}$ (m)	ε (%)	$H_{m,1}$ (m)	$H_{m,2}$ (m)	ε (%)
I-shaped	1	50 km	1.83	1.70	7.10	1.99	1.70	14.57
	2	50 km	4.17	3.59	13.91	2.30	2.22	3.50
T-shaped	1	50 km	2.71	2.34	13.65	2.56	2.18	14.84
	1	100 km	3.12	2.86	8.30	3.29	2.77	15.80

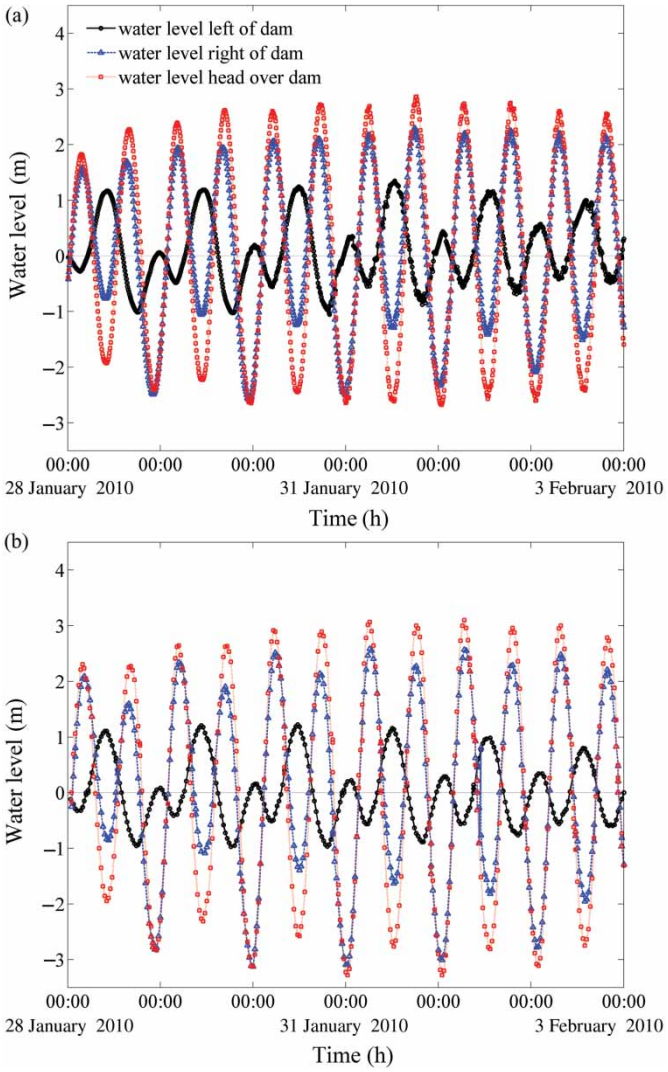

Figure 9 Variation of water level with time for 100 km T-shaped dam at Location 1: (a) present results and (b) previous results (Adema and Hartsuiker 2010)

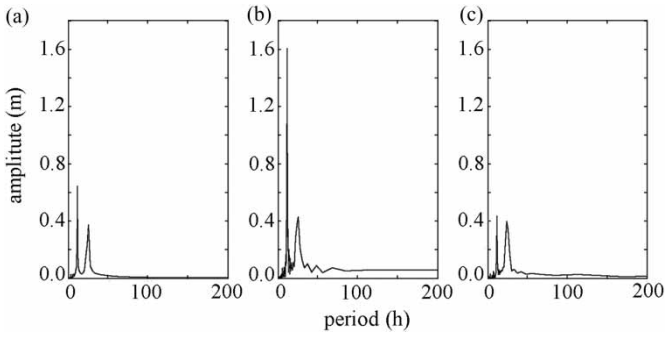

Figure 10 Frequency spectrums of tidal wave amplitudes at Location 1: (a) without a dam, (b) right side of I-shaped dam, and (c) left side of I-shaped dam

A comparison is carried out of the tidal wave behaviour in a marine environment between with and without a 50 km I-shaped dam at Location 1. Analysis of tidal wave amplitudes at this location with and without such a dam is performed in a frequency-domain and its results are shown in Fig. 10.

It can be seen from Fig. 10a that for the case without any dam there are two peaks at periods 12 and 24 h in the frequency spectrum curve. The peak values of the tidal wave amplitudes are 0.65 and 0.4 m, respectively. The first peak at the tidal wave period 12 h is about 1.6 times larger than the second one at period 24 h. It is also shown that amplitudes for period larger than 200 h are very small and can be neglected.

Once a 50 km I-shaped dam is constructed in the above-mentioned location, tidal waves around the dam undergo substantial changes and consequently such changes lead to the phase shift of the tidal waves on the left and right sides of the dam. The results on the variation of the tidal wave amplitude with period are shown in Fig. 10b and 10c. It can be seen from Fig. 10 that the second peak occurs at the tidal wave period 24 h varies slightly regardless of cases with or without a dam, and that the amplitude of semi-diurnal tidal wave (first peak) on the right side (facing flood) of the dam occurs at the tidal wave period 12 h.

It can be seen from Fig. 10b and 10c that for cases with a dam the amplitude of semi-diurnal tidal wave shows a big changes compared to that for cases without a dam as follows: the amplitude of semi-diurnal tidal wave on the right side (facing flood) of the dam, taking the largest percentage of the spectrum, is 1.6 m and almost 2.5 times larger than ones at the same site without dam, while the amplitude of semi-diurnal tide on the left side (facing ebb) decreases to about 0.4 m, resulting in a significant fall in the water surface level on the left side of the dam, and then a large water level difference between both sides of the dam appears.

3.4 *Effect of angle α*

To recognize the strength of wave focusing exhibited for a Y-shaped dam with different angles α, it is necessary to examine the influence of angle α on water head. A Y-shaped dam composed of a branch dam with length $L = 30$ km and a main dam with length $l = 50$ km at Location 1 is considered. The angle α varies from 0°, 30°, 45°, 60° to 90°. This includes two special cases, namely for $\alpha = 0°$ the dam would be I-shaped whereas for $\alpha = 90°$ the dam would be T-shaped.

Water surface levels on both sides of the dam and water heads for various angles α are shown in Fig. 11. Through the comparison of water levels for angle $\alpha = 0°$, 30°, 40°, 45°, 60° and 90° in the same time as shown in Fig. 11a–11f, respectively, the water surface levels vary with α whereas the phase shifts also vary with α.

The maximum water heads, average water heads, and average phase shifts for the Y-shaped dam with angle $\alpha = 0°$, 30°, 40°, 45°, 60° and 90° are tabulated in Table 3. It can be seen that the maximum water head is about 1.0–1.2 m higher than the average one. The phase shift for a Y-shaped dam varies between 1.250 and 1.474π regardless of α value. It can be seen that when α is 40°, the water head reaches a maximum, namely 2.694 m. It is found that when α is 40° the phase shift of the tidal waves on both sides of the dam is 1.250π, leading to a considerable water head.

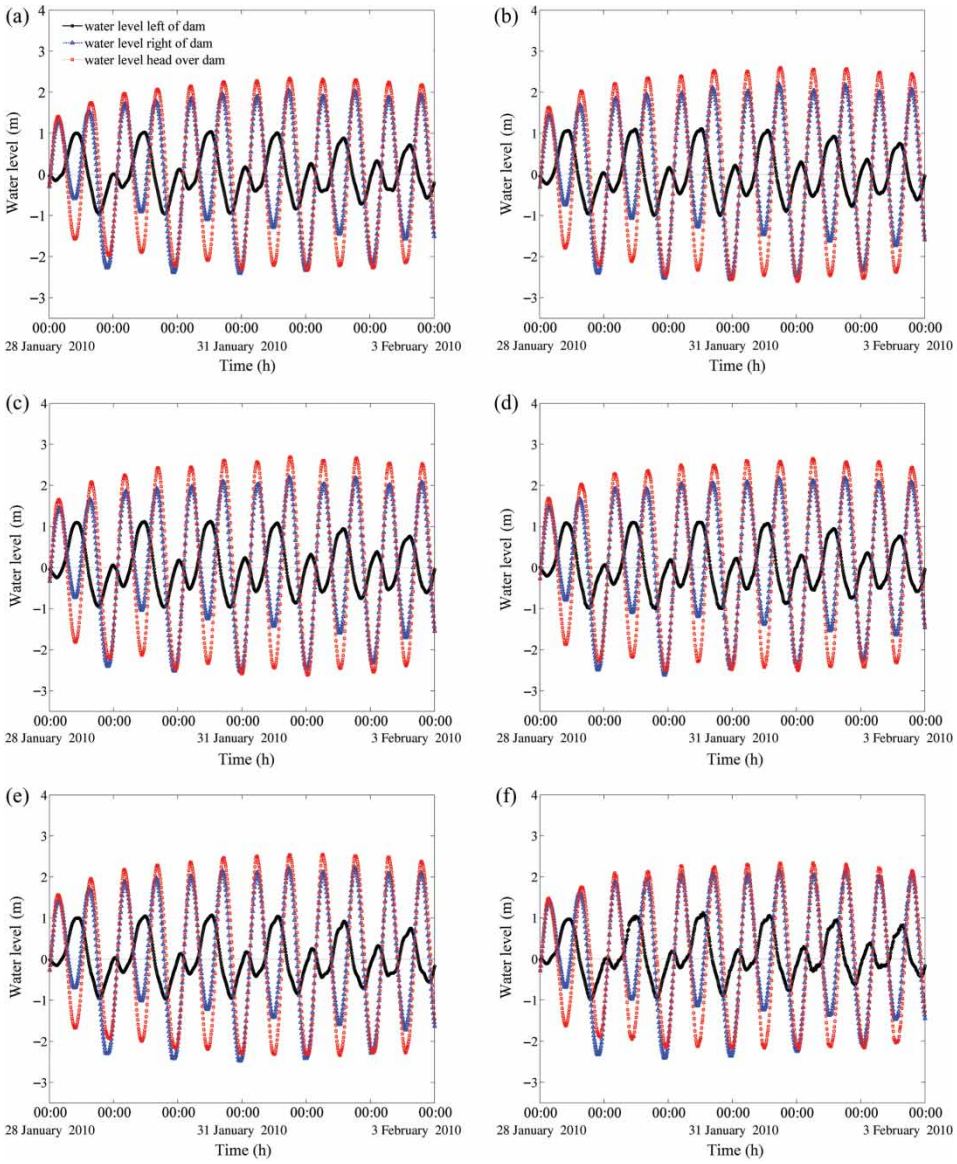

Figure 11 Variation of water levels with time for Y-shaped dam with various angle: (a) $\alpha = 0°$, (b) $\alpha = 30°$, (c) $\alpha = 40°$, (d) $\alpha = 45°$, (e) $\alpha = 60°$, and (f) $\alpha = 90°$

Table 3 Variation of water head and phase shift of the Y-shaped dam with α

$\alpha(°)$	Maximum head (m)	Average head (m)	Phase shift
0	2.341	1.336	1.330π
30	2.603	1.483	1.307π
40	2.694	1.517	1.250π
45	2.609	1.442	1.311π
60	2.548	1.409	1.409π
90	2.344	1.276	1.474π

The variation of water head and phase shift with angle is also shown in Fig. 12. It can be found that for angle $\alpha \in [0°, 40°]$, the bigger the angle is, the larger the maximum and average water heads are whereas for angle $\alpha \in [40°, 90°]$, the bigger the angle is, the smaller the maximum and average water heads are. It is clearly shown that when $\alpha = 40°$ the water head reaches the largest value, namely 2.694 m. For a Y-shaped dam, there always exists the largest water head after the optimization of α. These findings would be useful for guiding designers' attempts to optimize Y-shaped dam so as to obtain the maximum water head. It should be pointed out that a phase shift of 1.0π for regular sinusoidal or cosine waveform is optimal for maximal water head, whereas for real irregular tidal wave, the more close to 1.0π the phase shift is, the higher the water head is expected to be, as demonstrated in Fig. 12.

3.5 *Effect of branch dam length L*

Our previous discussion indicates that branch dam length plays a significant role in water heads. In order to see how L influences hydrodynamic characteristics of tidal waves, a wide range of L is examined. The physical and geometric parameters given in the previous section are used, but we vary L in order to understand

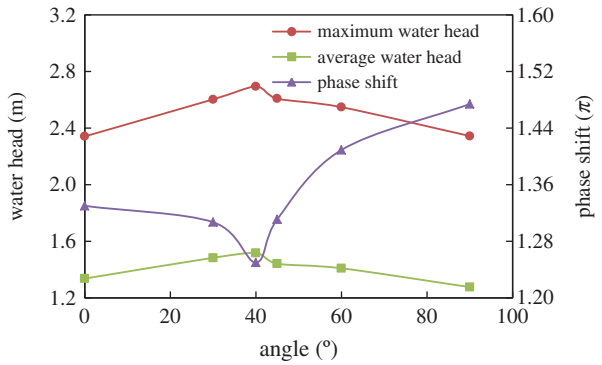

Figure 12 Variation of water head and phase shift with angle α

how discrepancies in phase shift of the tidal waves and water head are affected by different L. The angle α is fixed as 45°, while the branch dam length (Y-bar) varies from 15, 30, 45, 60, 90 to 120 km. Temporal variation of water surface levels at both sides of the dam and water heads for Y-shaped dam are shown in Fig. 13. Maximum water heads, average water heads, and average phase shifts for various branch dam lengths of Y-shaped dam are tabulated into Table 4.

Table 4 Maximum water head, average water head and average phase shift for various branch dam lengths of Y-shaped dam

L(km)	Maximum head (m)	Average head (m)	Phase shift
15	2.489	1.286	1.402π
30	2.667	1.488	1.363π
45	2.811	1.532	1.178π
60	2.922	1.598	1.228π
90	3.129	1.716	1.228π
120	3.168	1.763	1.206π

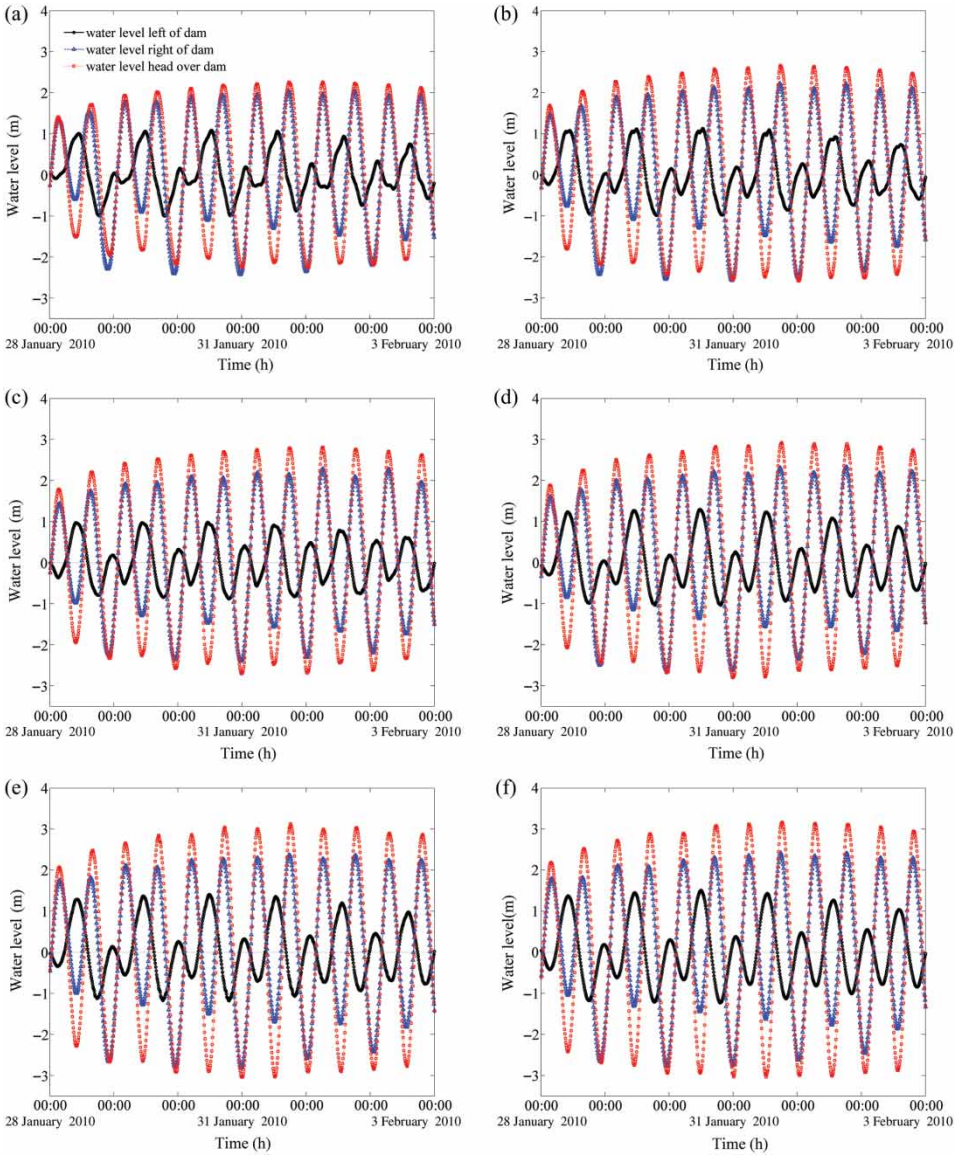

Figure 13 Variation of water level with time for Y-shaped dam with various dam length: (a) $L = 15$ km, (b) $L = 30$ km, (c) $L = 45$ km, (d) $L = 60$ km, (e) $L = 90$ km, and (f) $L = 120$ km

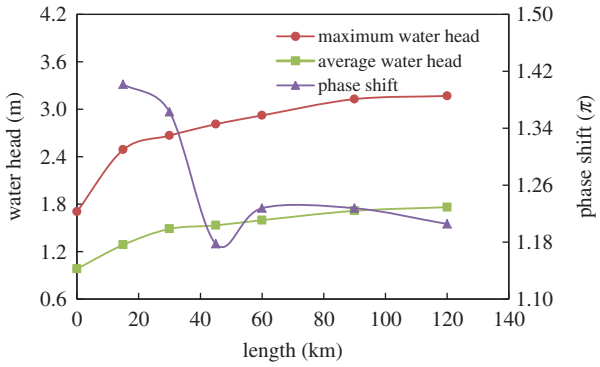

Figure 14 Variation of water head and phase shift with branch dam length L

Table 5 Water heads for two types of dams

Water head (m)	Y-shaped	T-shaped	ε_0 (%)
Maximum	2.609	2.344	11.30
Average	1.442	1.276	13.01

As Fig. 13 shows, water heads increase with increasing L almost at the same time, and the maximum water head changes from 1.705 m to about 3.168 m for the examined cases. As shown in Table 4 and Fig. 14, the maximum and average water heads increase with L, and the maximum water heads are about 0.7–1.4 m higher than the corresponding average water heads. It can be seen that average water head for $L = 120$ km is 15% larger than one for $L = 45$ km as L increasing by 167%, whereas average water head for $L = 90$ km is 12% smaller than one for $L = 45$ km as L increasing by 100%. For the former to increase L by 1% means to increase average water head by 0.09%, whereas for the latter to increase L also by 1% means to increase average water head by 0.12%. That does not mean the longer the better from an economic point of view. For $L = 45$ km the phase shift of the tidal wave on both sides of the dam is the smallest, namely 1.178π, as shown in Fig. 14.

3.6 *Effect of dam type*

The effect of dam type on the water head is also of interest. Water heads for two types of dams are calculated and shown in Table 5, where the relative difference defined by Eq. (5) is also given.

$$\varepsilon_0 = \frac{Y - T}{T} \times 100\% \tag{5}$$

where ε_0 is the relative difference, Y is the Y-shaped dam result, and T is the T-shaped dam result.

It can be seen from Table 5 that the maximum water head over the Y-shaped dam ($\alpha = 45°$) is 0.265 m (about 11.30%) higher than that over the T-shaped dam ($\alpha = 90°$), whereas the average water head is 0.166 m (about 13.01%) higher than that over the T-shaped dam. More considerable tidal power could be harnessed at the same construction expenditure with Y-shaped dam than T-shaped dam due to tidal power focusing of the Y-shaped dam probably due to the following reasons:

(1) The branch part of the Y-shaped dam helps to collect more tidal power with its geometrical narrowing by increasing the power density along with wave propagation, which can be defined as the tidal wave gathering effect;
(2) When geometrically appropriate, the inherent frequency of the water body inside the dam may become close to the tidal wave frequency, which can reinforce resonance of the water body.

Besides, when the length of the dam is appropriate, it happens that the water level on the left and right sides have nearly opposite phase, which means, when the water level on one side comes to the peak, the water level on another side comes to the bottom, providing a considerable and comparatively large water head.

4 Conclusions

In this paper, we investigate PSTP generated by a dam perpendicular to the coastline, which causes a phase shift in water level on the both sides of the dam. A Y-shaped dam consisting of a branch dam and a main dam is considered. The effects of branch dam length, angle between the main dam axis extension line and branch dam axis, and dam type on the water head and phase shift of the tidal wave are analysed by using a two-dimensional shallow water flow model.

It is found that when the angle $\alpha = 40°$, the phase shift of the tidal waves at both sides of the dam approaches 1.0π and the water heads acted over the Y-shaped dam reach the largest value. Water heads increase with increasing branch dam length L, as expected. For the branch dam length L, when L is about 30–45 km, nearly as long as the main dam, while the phase shift comes close to 1.0π, the water head gained is also considerable. A comparison between Y- and T-shaped dam is made to elucidate the difference in water heads acted over the dams. Results reveal that the Y-shaped dams have more advantage than the T-shaped ones in collecting tidal power mainly due to the fact that the special arrangement and geometrical parameters of Y-shaped dam may induce resonance of the water body nearby, and enhance the tidal power density or tidal wave gathering effect.

Further work will focus on parametric study on power generation for Y-shaped dams and evaluation of construction cost related to extension and water depth increment along with the ecological and environmental influence.

Funding

The research is supported by the National Natural Science Foundation of China [grant nos 51079072, 51279088], the national high technology research and development program [grant no. 2012AA052602], and

State Key Laboratory of Hydroscience and Engineering [grant no. 2013-KY-3].

Notation

B_x = baroclinic pressure gradient (m^2s^{-1})
B_y = baroclinic pressure gradient (m^2s^{-1})
D_x = lateral stress gradient (m^2s^{-1})
D_y = lateral stress gradient (m^2s^{-1})
f = $2\Omega \sin\varphi$ = Coriolis parameter (s^{-1})
g = gravitational acceleration (ms^{-2})
H ≡ $\zeta + h$ = total water column thickness (m)
h = bathymetric depth (m)
$H_{m,1}$ = maximum water head in previous study (m)
$H_{m,2}$ = maximum water head in the present study (m)
L = branch dam length (km)
l = main dam length (km)
P_s = atmospheric pressure at the sea surface (Pa)
Q_x, Q_y = UH, $VH = x$, y-directed flux per unit width, respectively (m^2s^{-1})
T = T-shaped dam result (m)
t = time (s)
U, V = depth-averaged velocities in the x, y direction (ms^{-1})
Y = Y-shaped dam result (m)
α = angel between the main dam axis extension line and branch dam axis (°)
γ = earth tide, self-attraction and load tide (m)
ε = relative error between the present numerical results and the previous results (–)
ε_0 = relative error between the Y- and T-shaped dam results (–)
ζ = free surface departure from the geoid (m)
η = Newtonian equilibrium tide potential (m)
ρ = time and spatially varying density of water due to salinity and temperature variations (kgm^{-3})
ρ_0 = reference density of water (kgm^{-3})
τ_{bx}, τ_{by} = bottom stress components (Pa)
τ_{sx}, τ_{sy} = imposed surface stresses components (Pa)
φ = latitude (°)

References

Adema, J., Hartsuiker, G. (2010). Potential location for dynamic tidal power in China. *Report No. C04021.002571*, Alkyon Hydraulic Consultancy and Research, Marknesse, The Netherlands.

Hulsbergen, K., Steijn, R., Hassan, R., Klopman, G., Hurdle, D. (2005). Dynamic tidal power (DTP). Proc. Int. Conf. *6th European Wave and Tidal Energy Conference*, Glasgow, UK, 215–221.

Hulsbergen, K., Steijn, R., Banning, G.V., Klopman, G., Fröhlich, A. (2008). Dynamic tidal power – a new approach to exploit tides. Proc. Int. Conf. *2nd International Conference on Ocean Energy*, Brest, France, 1–10.

Luettich, R.A., Westerink, J.J. (2004). *Formulation and numerical implementation of the 2D/3D ADCIRC finite element model version 44. XX*. Unc.edu, Morehead City, USA.

Matsumoto, K., Takanezawa, T., Ooe, M. (2000). Ocean tide models developed by assimilating TOPEX/POSEIDON altimeter data into hydrodynamic model: a global model and a regional model around Japan. *J. Oceanography* 56, 567–581.

Westerink, J.J., Blain, C.A., Luettich, R.A., Scheffner, N.W. (1994). ADCIRC: an advanced three-dimensional circulation code for shelves, coasts and estuaries, report 2: user's manual for ADCIRC-2DDI. *Dredging Research Program Technical Report DRP-92-6*, Army Engineers Waterways Experiment Station, Vicksburg, USA.

Zheng, S.M., Zhang, Y.L., Zhang, Q.H., Zhang, J.F. (2012). Numerical study on hydrodynamic characteristics of tide on both sides of T-type dam. *J. Hydroelectr. Eng.* 6, 179–185 (in Chinese).